ARMA 22-830

Osmotic Ion Concentration Control of Steady-State Subcritical Fracture Growth in Shale

Nguyen, Hoang T., and Bažant, Zdeněk P.
Northwestern University, Evanston, Illinois, USA

ABSTRACT: The mechanism of formation of natural cracks in sedimentary rocks in the geologic past is an important problem in hydraulic fracturing. Why are the natural cracks roughly parallel and equidistant, and why is the spacing in the order of 10 cm rather than 1 cm or 100 cm? Fracture mechanics alone cannot answer these questions. Here it is proposed that fracture mechanics must be coupled with the diffusion of solute ions (Na^+ and Cl^- are considered here), driven by an osmotic pressure gradient. Parallel equidistant cracks are considered to be subcritical and governed by the Charles-Evans law. The evolution in solute concentration also affects the solvent pressure in the pores and cracks, altering the resistance to frictional sliding. Only steady-state propagation and periodic cracks are studied. An analytical solution of the crack spacing as a function of the properties of the rock as well as the solvent and solute, and the imposed far-field deformation is obtained. Finally, the stability of the growth of parallel cracks is proven by examining the second variation of free energy. Stability of the periodic growth state is also considered.

1 INTRODUCTION

The deep layers of sedimentary rocks such as shale and sandstone are usually intersected by systems of nearly parallel natural cracks either filled by mineral deposits or closed by creep over a million year life span. Their spacing is roughly uniform and is on the order of 0.1 m (rather than 1 m or 0.01m). These cracks likely play an important role in hydraulic fracturing for gas or oil recovery (aka fracking, fraccing or frac) (Rahimi-Aghdam et al., 2019, e.g.). Therefore, understanding the mechanism of their formation in the distant geologic past is of interest.

What controls the spacing of the nearly parallel cracks in shale? According to the fracture mechanics alone, the crack spacing is arbitrary. If propagating parallel equidistant cracks are in a critical state, stability analysis shows that many cracks would have to stop growing, causing a great increase of their average spacing, which was obviously not the case (Bažant et al., 2014).

The main hypothesis advanced here is that cracks must be subcritical, propagating slowly, and that the spacing is controlled by the diffusion of fluids, due to a difference in solute concentration. In particular, it is proposed that the natural crack spacing is dictated by an osmotic pressure gradient which drives diffusion of solvents and solute ions (e.g., Na^+ and Cl^-) in the direction normal to the crack. Since the diffusion cannot be instantaneous, one must consider a slow subcritical crack propagation (Olson, 1993, 2004). Also note that this sustained growth would be feasible even when seismic and microseismic events were absent, as long as their residual effects remained. This constant activation could also explain why the hairline cracks maintain their permeability despite creep (Chau et al., 2017). Such cracks can keep growing for thousands, even millions, of years after a tectonic event.

In this study, the cracks are considered to grow at the typical depths of hydraulic fracture (about 3km). When the fracture process zone (FPZ) at the crack front advances (either by slipping or opening), it will also dilate. The dilation will dilute the concentration of solute ions within the FPZ and reduce the intensity of the stress-corrosion process, which slows down the crack growth. In addition, the drop of ionic concentrations compared to the adjacent rock and the semipermeable nature of the tight gas shale will cause a diffusion of the solvents out of the FPZ and of the solute from the FPZ towards the crack; see Fig. 1. This increases the pore pressure which in turn imposes a

compression on the crack surfaces and further inhibits the crack growth.

This work aims to propose an explanation for a dense network of cracks that can generate a large enough permeability within impermeable shale rock strata (Bažant et al., 2014). This dense network was shown to be necessary to promote branching in the hydraulic cracks, which ultimately lead to a high enough natural gas yield.

2 THE PROPAGATION OF A PARALLEL SYSTEM OF LONG MODE-I AND MODE-II FRICTIONAL CRACKS

Consider the typical depth of hydraulic fracture, 3 km. The horizontal mean tectonic stress at that depth is about 50 MPa. Such compression prevents the formation of Mode-I cracks, which would create an open space between crack surfaces. On the other hand, vertical Mode-III cracks propagating horizontally would imply implausibly large vertical sliding displacements. So the only plausible way to explain how parallel natural cracks formed millions years ago is to consider parallel mode-II cracks. If the crack faces are in sliding contact, the friction will impose a uniform field of residual shear stress.

Postponing the questions of crack spacing stability, we consider for simplicity that an infinite elastic space contains an infinite system of semi-infinite parallel cracks of uniform spacing $2s$, as shown in the horizontal section in Fig. 1. The infinite space is in the state of plane strain, which makes the problem two-dimensional (2D).The cracks and the entire space are subjected to far-field shear strain γ, which is presumably the residual deformation from a major tectonic event, and normal compressive stresses σ_H and σ_h which, at the depth of 3 km typical of shale fracking, approximately equal 50 MPa (equivalently, overall uniform far-field deformations, u and v, could be assumed).

The friction at the crack faces sliding against each other is $\tau_{fric} = k\sigma_N$, where k is the kinetic friction coefficient, for shale about 0.4 (Kohli and Zoback, 2013). At the front of each crack there is a fracture process zone (FPZ) of a certain characteristic length l_0 and finite width w_f. Note that these lengths on the same materials are different for cracks propagating at different modes, and mode-II cracks usually have higher fracture energy and hence a larger characteristic length. In this problem, we consider the case where the deformation state from one parallel crack to the next is periodic, and so we may analyze only one crack between two symmetry lines of periodicity.

We assume the periodic strata to have reached a (static) steady state of sliding velocity $\dot{u}$ and a crack tip propagation velocity $\dot{a}$, while frictional stress $k\sigma$ is acting on the crack faces ($\dot{u}$ = time rate of sliding displacement u). In the steady state, the deformation field and crack length must remain periodic, as shown in Fig. 1a.

A key hypothesis of the present analysis is the attainment of a steady state. It is characterized by vanishing rate of stress intensity factor or energy release rate; (Bažant and Planas, 1998):

$$\frac{\mathrm{d}\mathcal{G}}{\mathrm{d}t} = \dot{P}\left[\frac{\partial \mathcal{G}}{\partial P}\right]_{a=\text{const.}} + \dot{a}\left[\frac{\partial \mathcal{G}}{\partial a}\right]_{P=\text{const.}} = 0 \quad (1)$$

where P represents the generalized load (far-field stresses, strains, or displacements). Therefore, not only the generalized load P needs to be in a steady state (which is usually the case because the aftermath of a tectonic activity settles at a residual stress/strain field). Hence $\dot{a}$ should cause no change in K or $\mathcal{G}$. The solutions in (Tada et al., 2000) shows that this can be true only in the case of far-field tensile and shear strain (with and without friction). Far-field stresses, with and without the presence of friction, will always trigger a positive $\partial K/\partial a$.

3 THE GROWTH OF SUBCRITICAL CRACKS

The formation of natural cracks depends on the frequency and the magnitude of tectonic activities at the regions of interest. These activities, however, are not always seismic, and estimating a correct time scale will always result in a considerable error. However, one thing that we know from thermodynamic stability analysis is that, at the time of formation, the natural cracks in shale will localize into one or several major slipping faults, with short distributed cracks emanating from them (Gephart, 1990; Bazant and Tabbara, 1992).

The tips of the parallel cracks could not have been in a critical state in which $\mathcal{G} = \mathcal{G}_c$. Indeed, the peak magnitude of any tectonic activities lasts for only a short period of time and leaves behind a residual deformation. So the cracks must have grown slowly and statically under the effect of these residual strains. Such a slow subcritical crack growth generally follows the empirical Charles-Evans law (Charles, 1958):

$$\dot{a}/\dot{a}_0 = \kappa(c)\, e^{-Q/RT}\left(\frac{\mathcal{G}}{\Gamma_c}\right)^{n(c)/2} \quad (2)$$

where $\dot{a}_0$ = dynamic crack velocity, Q = activation energy of fracture (J/mol), T = absolute temperature, R = gas constant, n = subcritical index; n changes with the solute concentration, ranging from 4.8 ± 3.0 for deionized water to 13.8 ± 3.8 for water with 6.1 molarity (Chen

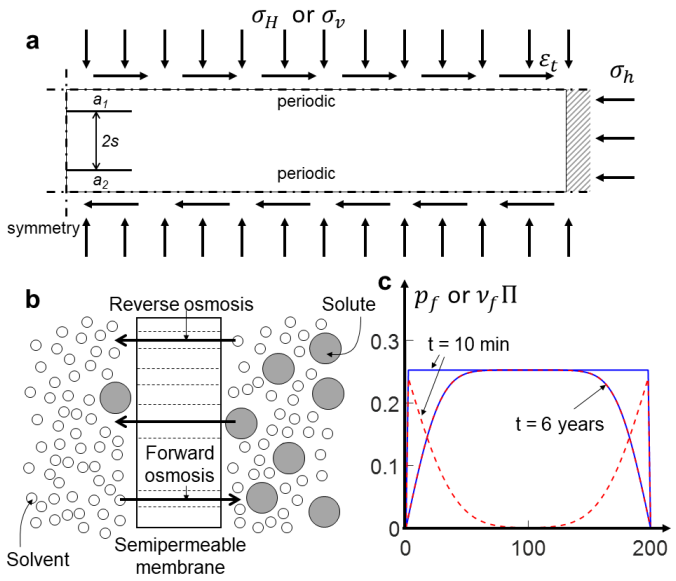

Fig. 1: a) The periodic parallel cracks are growing under the effect of subcritical far-field stresses or strains; b) While solvent particles can move freely across the semi-permeable membrane, a small amount of solute particles can pass through it, leading to an osmotic pressure; c) The evolution of solvent and osmotic pressure from steady to transient state where $p_f = \nu_f \Pi$.

et al., 2017). Here we divided n by 2 since this index is usually considered to be an exponent of stress intensity factor $K = \sqrt{E'\mathcal{G}}$; $E' = E/(1-\nu^2)$ as plane strain is here assumed, E = Young's modulus, and ν = Poisson ratio; κ is an empirical factor normally considered as 1, but for immersed shale we must consider it to depend on the concentration, c, of solute ions of various kinds, mainly NaCl (dissociated as Na^+ and Cl^-), and partly also KCl (Chen et al., 2017).

The dependence of κ and n in Eq. (2) on the solute concentration can be simplified using the first two terms of the Taylor series expansion:

$$\kappa(c) = \kappa_T + \kappa'_T(c - c_0);\ n(c) = n_T + n'_T(c - c_0) \qquad (3)$$

where c_0 = the concentration of solute ions inside the cracks, c = steady-state concentration of solute in the rock matrix ($c > 0$) and generally $\kappa'_T > 0$ because a higher ion concentration means a stronger stress corrosion effect ($c_0 \sim$ kg/m^3, n'_T and $\kappa'_T \sim$ m^3/kg, n_T and κ_T is dimensionless). The calibration of these constants is done based on the measurements by Chen et al. (2017).

4 STRESS INTENSITY FACTOR OF CRACKS SUBJECTED TO FAR-FIELD STRAINS AND FRICTIONAL CONTACT

The remaining unknown quantities in Eq. (2) are the energy release rate and the material fracture energy in each mode. The latter were reported by Rao et al. (2003); Pan et al. (2019); Li et al. (2019); Choo et al. (2021) for shale and other rocks. We consider first the stress intensity factor for far-field strains (Tada et al., 2000; Rice, 1967; Knauss, 1966). In these two cases, the stress intensity factors both reach an asymptotic value with $\partial K/\partial a = 0$.

$$K_I = E\epsilon_n\sqrt{s/(1-\nu^2)} \qquad (4)$$

$$K_{II} = G\gamma_t\sqrt{2s/(1-\nu)} \qquad (5)$$

We note that, under the confining field of normal stress and strain, a mode I crack is enabled to form only at an inclination to the minimum principal stress direction.

Let us now consider the effect of friction on the effective mode II stress intensity factor (Rao et al., 2003):

$$K_{II}^{eff} = K_{II} - k\langle -K_I\rangle \qquad (6)$$

where the Macaulay bracket $\langle\rangle$ in the foregoing equation reflects the fact that only the compressive normal stress imposes a residual stress τ_r against mode-II propagation. The effective mode II stress intensity factor is then written as:

$$K_{II}^{eff} = G\gamma_t\sqrt{\frac{2s}{1-\nu}} - kE\langle -\epsilon_n\rangle\sqrt{\frac{s}{1-\nu^2}} \qquad (7)$$

We note that the second term in Eq. (7) is non-zero only when $\epsilon_n < 0$. Note that, Eq. 7 was confirmed by Palmer and Rice (1973) for mode II stress intensity factor of overconsolidated clay, which can be written as $G(\gamma_t - \gamma_r)\sqrt{2s/(1-\nu)}$. Therefore, the shear stress τ_{fric} that is required for steady-state sliding of the crack faces is equivalent to:

$$\tau_{fric} = G\gamma_r < \gamma_t \qquad (8)$$

Here the residual strain γ_r depends on the applied normal stress at the crack surfaces, the elastic properties and the friction coefficient between the surfaces of shale. For velocities encountered in mechanical processes (> 1 m/s), k is known to depend on the state variables and sliding velocity (Ruina, 1983; Rice et al., 2001) but it is likely that the velocity dependence becomes negligible within the range of geological sliding velocities, such as 0.1 m/year.

5 THE EFFECT OSMOTIC PRESSURE OF SOLUTE PARTICLES AND SOLVENT TRANSPORT

When a crack propagates, its dilation will trigger the movement of solute and solvent molecules. When the ions are allowed to move freely, the solute concentration must follow Fick's law (Fick, 1855), whose molecular mechanism is the random Brownian motion of solute and solvent

atoms. However, the nanoporous structure in shale creates a distributed semipermiable 'membrane' that is almost impassable by the solute molecules. Therefore, only pores on the order of ten to a hundred nanometers will allow solute molecules to pass through them. Consequently, the majority of solute particles have to stay put in the larger pores or move relatively much more slowly compared with the solvent molecules. Therefore, the molar concentration, n_c, of the solute ions per unit volume of porous medium must remain constant or evolve slowly. The concentration of the solvent (water), however, changes faster due to an easier diffusion through the pores.

In the structure of shale, these semipermeable "membranes" are distributed within the body of the material, causing a gradient in solute concentration. This contrasts with the familiar thin membranes used for desalination, in which the concentration drops by a jump. This kind of diffusion consists of movement of the molecules of the solvent, i.e., water, through the a system of nanopores in shale. The governing equation for this transport is (Leng et al., 2021):

$$q_w = -\frac{\chi}{\mu}(\nabla p_f - \nu_f \nabla \Pi) \quad \text{where } \Pi = 2RTc \tag{9}$$

Here χ = permeability (of the solvent)μ = dynamic viscosity of the solvent, and ν_f = osmotic efficiency, about 0.96 for shale, which is close to full efficiency 100%. The signs in Eq. (9) represent two opposite flows. Water flows from higher to lower p_f but from lower to higher c. The condition of mass conservation reads (Leng et al., 2021):

$$\frac{\partial \zeta}{\partial t} = -\nabla \cdot q_w \tag{10}$$

where ζ = divergence of the solvent displacement = outflow of solvent (i.e., water) volume from a unit element of shale. So, the governing partial differential equation is (Leng et al., 2021):

$$c_t \frac{\partial p_f}{\partial t} = \frac{\chi}{\mu}\left(\nabla^2 p_f - 2\nu_f RT \nabla^2 c\right) \tag{11}$$

Π represents the pressure increase of the solvent, i.e., water, that is required for passage through the confined spaces, the nanopores. $c_t = 1/M_B + \zeta_0/K_f$ is the total compressibility of the pore space (contributed mainly by the compressibility of the larger pores), M_B is Biot's modulus (defined by $1/M_B = \partial\phi/\partial p_f$ at constant solvent density) and K_f is the solvent bulk modulus (defined by $1/K_f = 1/\rho_f \partial\rho_f/\partial p_f$ at constant pore volume).

To calculate the profile of concentration (or molarity) of solute particles, c, (NaCl, mainly) in a steady-state flow, we consider the following equation (Leng et al., 2021):

$$q_s = -(1-\nu_f) D_e \nabla c \tag{12}$$

where q_s is the volumetric flux of the solute particle per a unit volume of solvent and D_e is the intrinsic diffusion coefficient of ions in solvent according to Fick's law, generated by the Brownian motion of both solute and solvent particles. This diffusion, however, is hindered by the semipermeable nature of the shale strata. Ideally, if all of the pore diameters are smaller than the mean free path of the solute particles, $\nu_f = 1$, this transport is totally inhibited. But in reality, the pore size distribution varies among shales and sedimentary rocks, and larger pores will allow the solute to pass through ($\nu_f < 1$). Therefore, this value can range from 10^{-3} to 10^{-1} (Horseman et al., 2007; Takeda et al., 2014) to close to 1 (Marine and Fritz, 1981). The mass balance law for solute concentration reads:

$$\frac{\partial c}{\partial t} = -\nabla \cdot q_s \tag{13}$$

When the crack grows, the change in pores causes the dilation of the shale matrix between the cracks. Assuming that the diffusion is one dimensional, the maximum of the profile is attained at the tip of the crack and diminishes gradually behind the crack tip; see Fig. 1. The length of this region and the spatial distribution of pressure profile within it depends on the apparent diffusion coefficient of the solute and reaches a steady state as $\nabla p_f = \nu_f \nabla \Pi$. The increase of pore pressure due to the displacement of solvent molecules enhances the normal stress at the contacting surfaces, which in turn enhances the friction between them and reduce the effective stress intensity factor.

Using the foregoing equations, we can compute the concentration and pressure profiles and the modified effective stress intensity factor. Substituting the properties of some shale reservoirs (Morsy and Sheng, 2014; Chen et al., 2017; Leng et al., 2021), the typical spacing of parallel cracks is presented in Table **??**:

6 STABILITY OF STEADY-STATE CRACK GROWTH: CAN THE PARALLEL CRACKS GROW FOREVER?

In the previous section, we concluded that the anticipated spacing can be possible under certain circumstances. However, that is only the steady-state solution. The path that leads to that spacing, from an initial distribution of crack, has still been unclear. To see how the cracks propagate, we consider the simplified case that is composed of 2 cracks with initial length a_1 and a_2 with distance $2s$. The velocity of each crack can be described, with non-zero energy release rate (e.g. $0 < \mathcal{G} < \Gamma_c$), by the Charles-Evans

Table 1: Typical material properties of Woodford shale and the calculated spacing

	Woodford	Barnett
ϕ_0	0.1 - 0.31	0.05 - 0.15
$\mu(cP)$	0.74-0.89	0.74-0.89
$\chi(\mu\text{Darcy})$	0.01-1	0.025-5
$c_t(\text{GPa}^{-1})$	0.51	1.25
ν_f	1	0.96
T (K)	300	300
R	8.314	8.314
Depth (m)	2500-3600	2900-3200
$\dot{a}_0(\mu m/s)$	45-60	23.5-76.5
$c_0(kg/m^3)$	0.2-0.3	0.15-0.4
Calculated spacing (cm)	7.5-20.2	5.4-30.5

law (Charles, 1958):

$$\dot{a}_1 = C/\Gamma_c^m \mathcal{G}_1^m(a_1,a_2) = \mathcal{F}_1(a_1,a_2) \quad (14)$$

$$\dot{a}_2 = C/\Gamma_c^m \mathcal{G}_2^m(a_1,a_2) = \mathcal{F}_2(a_1,a_2) \quad (15)$$

where $C = \dot{a}_0 \kappa(c)\, e^{-Q/RT}$, Γ_c and $m = n/2$ were mentioned in previous sections. Thus we have a system of nonlinear ordinary differential equation in time. The stability of the uniform crack growth (or any solution path) can be considered by the linearization around a solution point:

$$\dot{a}_1 = \mathcal{F}_1 + \frac{\partial \mathcal{F}_1}{\partial a_1}(a_1 - a_{10}) + \frac{\partial \mathcal{F}_1}{\partial a_2}(a_2 - a_{20}) + O(\delta^2 \mathcal{F}_1) \quad (16)$$

$$\dot{a}_2 = \mathcal{F}_2 + \frac{\partial \mathcal{F}_2}{\partial a_1}(a_1 - a_{10}) + \frac{\partial \mathcal{F}_2}{\partial a_2}(a_2 - a_{20}) + O(\delta^2 \mathcal{F}_2) \quad (17)$$

where a_{10}, a_{20} is any solution point within the admissible domain. The nonlinear problem is now turned into a linear problem with the variable $\tilde{a} = a - a_0$. This can then be rewritten as:

$$\begin{Bmatrix} \dot{\tilde{a}}_1 \\ \dot{\tilde{a}}_2 \end{Bmatrix} = \tilde{C} m \begin{bmatrix} \mathcal{G}_1^{m-1}\mathcal{G}_{1,1} & \mathcal{G}_1^{m-1}\mathcal{G}_{1,2} \\ \mathcal{G}_2^{m-1}\mathcal{G}_{2,1} & \mathcal{G}_2^{m-1}\mathcal{G}_{2,2} \end{bmatrix} \begin{Bmatrix} \tilde{a}_1 \\ \tilde{a}_2 \end{Bmatrix} = \begin{bmatrix} \mathcal{F}_{1,1} & \mathcal{F}_{1,2} \\ \mathcal{F}_{2,1} & \mathcal{F}_{2,2} \end{bmatrix} \begin{Bmatrix} \tilde{a}_1 \\ \tilde{a}_2 \end{Bmatrix} \quad (18)$$

Here $\tilde{C} = C/(\Gamma_c)^m$. Note that, if the equal-length crack growth is being considered, due to the symmetry of the problem, $\mathcal{G}_1 = \mathcal{G}_2$; $\mathcal{G}_{1,1} = \mathcal{G}_{2,2}$; $\mathcal{G}_{1,2} = \mathcal{G}_{2,1}$. The solution of this problem will have the form:

$$\tilde{a} = c_1 e^{\lambda_1 t} v_1 + c_2 e^{\lambda_2 t} v_2 \quad (19)$$

where λ_1, λ_2 and v_1, v_2 are eigenvalues and eigenvectors of Eq.(18).

In Eq. (18), if we call $\tau = 2\mathcal{F}_{1,1}$, $\Delta = \mathcal{F}_{1,1}^2 - \mathcal{F}_{1,2}^2$. Several cases can be listed:

- If $\Delta < 0$, then the eigenvalues are real with opposite signs.
- If $\tau^2 < 4\Delta$, then the eigenvalues are complex with real part.
- If $\tau = 0$, $\Delta > 0$, then the eigenvalues are purely imaginary.
- If $\Delta > 0$, then the eigenvalues are real with opposite signs.

The linearized version will, therefore, be able to predict whether two cracks having equal-length can both sustain their propagation if there is a linear perturbation. As $t \to \infty$, the behavior of the solution will follow the direction of the eigenvector associated with the larger positive eigenvalue. Hence, we can check if a slightly uneven length can produce the divergence from the main propagation direction $a_1 = a_2$, which corresponds to the eigenvector {1,1}, or if one crack would start to propagate with a slightly longer length than another, corresponding to the eigenvector {1,-1}.

As mentioned, i.e. $\mathcal{G}_{1,1} = \mathcal{G}_{2,2}$, $\mathcal{G}_{1,2} = \mathcal{G}_{2,1}$, there will be two main eigenvectors $\{1,1\}$ and $\{1,-1\}$. Unlike the case of critical cracks, $\{1,-1\}$ is still an admissible direction, due to the initial non-zero velocity.

$$\begin{aligned} \dot{a}_1 - \dot{a}_0 &= \dot{a}_0 \\ \dot{a}_2 - \dot{a}_0 &= -\dot{a}_0 \\ \dot{a}_1 &= 2\dot{a}_0 \\ \dot{a}_2 &= 0 \end{aligned} \quad (20)$$

This case corresponds to a case of one crack decelerating and another extending to a longer length;

$$\begin{aligned} \dot{a}_1 - \dot{a}_0 &= \dot{a}_0 \\ \dot{a}_2 - \dot{a}_0 &= \dot{a}_0 \\ \dot{a}_1 &= 2\dot{a}_0 \\ \dot{a}_2 &= 2\dot{a}_0 \end{aligned} \quad (21)$$

Fig. 2 shows that, under the effect of the far-field deformation only, a system of subcritical cracks will localize into fewer and fewer cracks with accelerating speed. However, if a diffusion of solvent exists, the longer crack will trigger the foregoing mechanisms that reduce the stress intensity factor and enhance the fracture energy of the material locally at the tip. Therefore, the leading cracks will therefore decelerate, and no localization will happen.

REFERENCES

1. Bažant, Z. P. and Planas, J. (1998). *Fracture and Size Effect in Concrete and Other Quasibrittle Materials*. New Directions in Civil Engineering. CRC Press, Boca Raton and New York.

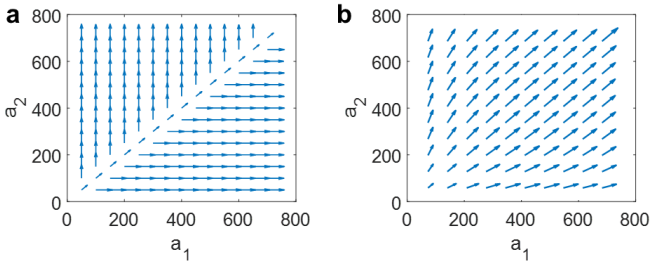

Fig. 2: a) Parallel sub-critical cracks will localize only when subjected to the far-field deformation and friction based on input data for Woodford shale (Morsy and Sheng, 2014; Chen et al., 2017); b) However, they will continue to grow together if the water diffusion and osmotic pressure are present.

2. Bažant, Z. P., Salviato, M., Chau, V. T., Viswanathan, H., and Zubelewicz, A. (2014). Why fracking works. *Journal of Applied Mechanics*, 81(10).

3. Bazant, Z. P. and Tabbara, M. R. (1992). Bifurcation and stability of structures with interacting propagating cracks. *International journal of fracture*, 53(3):273–289.

4. Charles, R. (1958). Dynamic fatigue of glass. *Journal of Applied Physics*, 29(12):1657–1662.

5. Chau, V. T., Li, C., Rahimi-Aghdam, S., and Bažant, Z. P. (2017). The enigma of large-scale permeability of gas shale: pre-existing or frac-induced? *Journal of Applied Mechanics*, 84(6).

6. Chen, X., Eichhubl, P., and Olson, J. E. (2017). Effect of water on critical and subcritical fracture properties of woodford shale. *Journal of Geophysical Research: Solid Earth*, 122(4):2736–2750.

7. Choo, J., Sohail, A., Fei, F., and Wong, T.-f. (2021). Shear fracture energies of stiff clays and shales. *Acta Geotechnica*, 16(7):2291–2299.

8. Fick, A. (1855). V. on liquid diffusion. *The London, Edinburgh, and Dublin Philosophical Magazine and Journal of Science*, 10(63):30–39.

9. Gephart, J. W. (1990). Stress and the direction of slip on fault planes. *Tectonics*, 9(4):845–858.

10. Horseman, S., Harrington, J., and Noy, D. (2007). Swelling and osmotic flow in a potential host rock. *Physics and Chemistry of the Earth, Parts A/B/C*, 32(1-7):408–420.

11. Knauss, W. G. (1966). Stresses in an infinite strip containing a semi-infinite crack.

12. Kohli, A. H. and Zoback, M. D. (2013). Frictional properties of shale reservoir rocks. *Journal of geophysical research: solid earth*, 118(9):5109–5125.

13. Leng, J., Lin, X., and Wang, L. (2021). Effects of osmosis on darcy flow in shales. *Energy & Fuels*, 35(6):4874–4884.

14. Li, W., Jin, Z., and Cusatis, G. (2019). Size effect analysis for the characterization of marcellus shale quasi-brittle fracture properties. *Rock Mechanics and Rock Engineering*, 52(1):1–18.

15. Marine, I. W. and Fritz, S. J. (1981). Osmotic model to explain anomalous hydraulic heads. *Water Resources Research*, 17(1):73–82.

16. Morsy, S. and Sheng, J. (2014). Effect of water salinity on shale reservoir productivity. *Advances in Petroleum Exploration and Development*, 8(1):9–14.

17. Olson, J. E. (1993). Joint pattern development: Effects of subcritical crack growth and mechanical crack interaction. *Journal of Geophysical Research: Solid Earth*, 98(B7):12251–12265.

18. Olson, J. E. (2004). Predicting fracture swarms–the influence of subcritical crack growth and the crack-tip process zone on joint spacing in rock. *Geological Society, London, Special Publications*, 231(1):73–88.

19. Palmer, A. C. and Rice, J. R. (1973). The growth of slip surfaces in the progressive failure of over-consolidated clay. *Proceedings of the Royal Society of London. A. Mathematical and Physical Sciences*, 332(1591):527–548.

20. Pan, R., Zhang, G., Xing, Y., Li, S., Zheng, X., and Tang, M. (2019). The experimental study of the shale bedding impact on fracture energy anisotropy. In *53rd US Rock Mechanics/Geomechanics Symposium*. OnePetro.

21. Rahimi-Aghdam, S., Chau, V.-T., Lee, H., Nguyen, H., Li, W., Karra, S., Rougier, E., Viswanathan, H., Srinivasan, G., and Bažant, Z. P. (2019). Branching of hydraulic cracks enabling permeability of gas or oil shale with closed natural fractures. *Proceedings of the National Academy of Sciences*, 116(5):1532–1537.

22. Rao, Q., Sun, Z., Stephansson, O., Li, C., and Stillborg, B. (2003). Shear fracture (mode ii) of brittle rock. *International Journal of Rock Mechanics and Mining Sciences*, 40(3):355–375.

23. Rice, J. (1967). Stresses in an infinite strip containing a semi-infinite crack. *Trans. ASME, Ser. E, J. Appl. Mech.*, 34:248–250.

24. Rice, J. R., Lapusta, N., and Ranjith, K. (2001). Rate and state dependent friction and the stability of sliding between elastically deformable solids. *Journal of the Mechanics and Physics of Solids*, 49(9):1865–1898.

25. Ruina, A. (1983). Slip instability and state variable friction laws. *Journal of Geophysical Research: Solid Earth*, 88(B12):10359–10370.

26. Tada, H., Paris, P. C., and Irwin, G. R. (2000). *The Stress Analysis of Cracks Handbook, Third Edition*. ASME Press.

27. Takeda, M., Hiratsuka, T., Manaka, M., Finsterle, S., and Ito, K. (2014). Experimental examination of the relationships among chemico-osmotic, hydraulic, and diffusion parameters of wakkanai mudstones. *Journal of Geophysical Research: Solid Earth*, 119(5):4178–4201.